JOURNAL OF COMPUTATIONAL PHYSICS 75, 151–167 (1988)

Analysis of Material Interface Discontinuities and Superconvergent Fluxes in Finite Difference Theory

R. J. MACKINNON AND G. F. CAREY

Department of Aerospace Engineering and Engineering Mechanics, The University of Texas at Austin, Austin, Texas 78712

Received July 11, 1986; revised April 10, 1987

An analysis of material interface discontinuities is developed and applied in finite difference theory to determine mathematically rigorous averaging techniques for material properties. This result is compared with other averaging techniques, particularly harmonic averaging, which is often applied in practice. We also develop a class of formulas of high accuracy for post-processing the difference formula to compute derivatives (fluxes, stresses), and conduct supporting numerical studies.

INTRODUCTION

Problems involving dissimilar materials frequently arise in solid mechanics, porous media flow, heat transfer, and many other scientific disciplines. At interfaces between materials, the material properties (elastic moduli, permeability, conductivity, etc.) are discontinuous. The governing conservation principles require that the flux be continuous across these discontinuity interfaces. In a variational formulation the interface is treated as an internal boundary, and flux continuity follows from the variational statement as a natural "boundary" condition. This implies in the associated finite element model, if element boundaries are aligned along the interface, that flux continuity is enforced approximately (see, e.g., Carey and Oden [6]). Moreover, the global rates of convergence remain optimal, whereas they are suboptimal if the element boundary does not coincide with the interface (Babuska [2]).

Finite difference theory does not implicitly offer such a "natural" mechanism for enforcing flux conservation at interfaces. The question of stability and convergence of difference schemes with discontinuous coefficients is examined in (Tikhonov and Samarski [12]). In practice, finite difference discretizations are frequently employed in which the mesh is constructed such that the discontinuity interface falls between adjacent nodes. The effect of the jump in material modulus is then accommodated by using a mean modulus such as the harmonic, arithmetic, or geometric mean for the subinterval containing the interface. Similar ideas have been applied in finite volume methods for flux balance in one dimension (Aziz and Settari [1] and Patankar [11]).

In the present study, we develop a finite difference analysis for the treatment of

0021-9991/88 $3.00

the interface. We begin by developing a class of formulas of high-order accuracy for the flux at any point and then consider the flux jump at the interface. The difference equation may be deduced from this analysis and then, using "condensation," a mathematical representation is derived which can be compared with the averaging strategies encountered in practice. We also observe that the analysis leads to a post-processing procedure for computing the flux to high accuracy. This result is analogous to that encountered in the superconvergent flux theory for finite elements (see, e.g., Wheeler [13], Dupont [8], Carey [4], Carey *et al.* [5]).

1. One-Dimensional Analysis

1.1. *Flux Representation*

We begin with a very simple case to introduce the main ideas. Consider a one-dimensional domain with interface at $x=\bar{x}$ and material property $k=k_1$ for $x<\bar{x}$ (Ω_1), $k=k_2$ for $x>\bar{x}$ (Ω_2) with $k_1 \neq k_2$ constants. The governing equation is

$$-(ku')' + bu = f \qquad \text{in } \Omega_1 \text{ and } \Omega_2 \tag{1}$$

with k given above and b, f sufficiently smooth functions. In addition, we require the usual interface conditions

$$[\![u]\!] = 0, \qquad [\![ku']\!] = 0 \qquad \text{at} \quad x=\bar{x}, \tag{2}$$

where $[\![\cdot]\!]$ denotes the "jump."

Let x^* be any point x in the domain (including $\bar{x}$). Expanding the (assumed known) solution u in a Taylor series about x^*, for arbitrary point $x=x^*+\delta$, we have

$$u(x^*+\delta) = u(x^*) + \delta u'(x^*) + \frac{\delta^2}{2!}u''(x^*) + \frac{\delta^3}{3!}u'''(x^*) + \cdots. \tag{3}$$

Let $\sigma = -ku'$ denote the flux. Then, from (3),

$$\sigma(x^*) = \frac{ku(x^*) - ku(x^*+\delta)}{\delta} + \frac{\delta}{2}ku''(x^*) + O(\delta^2) \tag{4}$$

and using (1),

$$\sigma(x^*) = \frac{k[u(x^*) - u(x^*+\delta)]}{\delta} + \frac{\delta}{2}(b(x^*)\,u(x^*) - f(x^*)) + O(\delta^2). \tag{5}$$

Thus, the truncated expression on the right yields a second-order accurate approximation to the flux at x^*.

The above result holds for $x^*=\bar{x}$ since the one-sided derivatives of u in the

Taylor-series expansion are well defined. Moreover, repeated differentiation of (1) can be used to generate successively higher order approximations to $\sigma(x^*)$.

1.2. *Interface Treatment*

Let $\delta = -\delta_1$, $\delta = +\delta_2$ (with $\delta_1, \delta_2 > 0$) define the points $x^* - \delta_1$, $x^* + \delta_2$ so that from (5)

$$\begin{aligned}\sigma_-(x^*) &= k_- \frac{[u(x^*-\delta_1)-u(x^*)]}{\delta_1} - \frac{\delta_1}{2}(b(x^*)\,u(x^*)-f(x^*)) + O(\delta_1^2)\\ \sigma_+(x^*) &= k_+ \frac{[u(x^*)-u(x^*+\delta_2)]}{\delta_2} + \frac{\delta_2}{2}(b(x^*)\,u(x^*)-f(x^*)) + O(\delta_2^2).\end{aligned} \tag{6}$$

Then

$$\begin{aligned}[\![\sigma(x^*)]\!] = \frac{k_-}{\delta_1}u(x^*-\delta_1) - \left(\frac{k_+}{\delta_2}+\frac{k_-}{\delta_1}\right)u(x^*) + \frac{k_+}{\delta_2}u(x^*+\delta_2)\\ -(b(x^*)\,u(x^*)-f(x^*))(\delta_2+\delta_1)/2 + O(\delta_1^2, \delta_2^2).\end{aligned} \tag{7}$$

For $x^* \neq \bar{x}$, $k_- = k_+$; for $x^* = \bar{x}$, then $k_- = k_1$ $k_+ = k_2$, and the condition $[\![\sigma]\!] = 0$ is approximated to order $O(\delta_1^2, \delta_2^2)$ by the "difference" expression on the right in (7). If $\delta_1 = \delta_2 = h$ then $[\![\sigma]\!] = 0$ is approximated to $O(h^3)$ since the second-order term now cancels.

2. Discrete Problem

2.1. *Difference Equations*

For the discrete problem, we locate grid points $\{x_i\}$, $i = 1, 2, \ldots, N$ in the domain. Setting $x^* = x_i$, $x^* - \delta_1 = x_{i-1}$, and $x^* + \delta_2 = x_{i+1}$ in (7), we have the representation for the analytic solution

$$\begin{aligned}[\![\sigma(x_i)]\!] = \frac{k_-}{\delta_1}u(x_{i-1}) - \left(\frac{k_+}{\delta_2}+\frac{k_-}{\delta_1}\right)u(x_i) + \frac{k_+}{\delta_2}u(x_{i+1})\\ -(b(x_i)\,u(x_i)-f(x_i))(\delta_2+\delta_1)/2 + O(\delta_1^2, \delta_2^2) = 0.\end{aligned} \tag{8}$$

From (8), by inspection, we may identify

$$\frac{k_-}{\delta_1}u_{i-1} - \left(\frac{k_+}{\delta_2}+\frac{k_-}{\delta_1}\right)u_i + \frac{k_+}{\delta_2}u_{i+1} - \frac{1}{2}(b_i u_i - f_i)(\delta_2+\delta_1) = 0 \tag{9}$$

as the standard 3-point difference scheme for (1) in the interior of Ω_1 or Ω_2 or at the interface $x_i = \bar{x}$ with $k_- = k_1$ and $k_+ = k_2$ as before. Note, however, that $\{u_i\}$ in (9) are now the difference solution values, not the exact values $u(x_i)$.

2.2. *Flux Calculation*

Further, formula (5) provides a scheme for accurately post-processing the flux. That is, using the solution $\{u_i\}$ to (9), we may compute the approximate flux at any grid point x_i as

$$\sigma_i = \frac{k}{\delta_2}(u_i - u_{i+1}) + \frac{\delta_2}{2}(b_i u_i - f_i), \tag{10}$$

where the usual divided difference expression is augmented by the additional correction term for greater accuracy. The higher order postprocessing schemes follow similarly (as in Appendix 1).

Remark. (i) If the boundary flux at one end is specified as data for problem (1), say $\sigma(1) = \gamma$, then we can use (10) or the higher order formulas to discretize this boundary condition more accurately in constructing the full set of difference equations for this Neumann problem; (ii) in special cases (e.g., $b = 0$, k, f constants), the solution to (9) is exact at the grid points (e.g., see Carey and Oden [7]), i.e., $u(x_i) = u_i$ and it follows immediately from (5) that flux formula (10) is $O(\delta^2)$ accurate. For more general k, b, f, there are error estimates for grid point and flux values in finite difference analysis (e.g., see Bramble and Hubbard [3]). These can also be applied in an analysis of the present flux formula (10) to prove $O(\delta^2)$ accuracy, and a proof will appear in a following paper (MacKinnon and Carey [10]).

2.3. *Condensation*

We see from (8) and (9) that if $\bar{x}$ is at a node, then the flux condition is satisfied approximately by the difference solution. We may treat the case where $\bar{x}$ is not at a node by introducing a temporary node at $\bar{x}$ and then eliminating (condensing) the associated equation. Let $x_{i+1/2} = \bar{x}$ denote the temporary node location and assume, for algebraic convenience, that b is constant. From (8) at $x_{i+1/2}$, setting $\delta = (\delta_1 + \delta_2)/2$,

$$\frac{k_1}{\delta_1} u(x_i) - \left(\frac{k_1}{\delta_1} + \frac{k_2}{\delta_2}\right) u(x_{i+1/2}) + \frac{k_2}{\delta_2} u(x_{i+1}) - \delta(bu(x_{i+1/2}) - f(x_{i+1/2})) + O(\delta^2) = 0. \tag{11}$$

Solving for $u(x_{i+1/2})$ and substituting in the equation for node i,

$$\frac{-k_1k_2(u(x_{i+1})-u(x_i))}{k_2\delta_1+k_1\delta_2+\delta_1\delta_2\bar{\delta}b}+\frac{k_1}{h_i}(u(x_i)-u(x_{i-1}))$$
$$+bu(x_i)\left[\frac{h_i+\delta_1}{2}+\frac{k_1\delta_2\bar{\delta}}{k_2\delta_1+k_1\delta_2+\delta_1\delta_2\bar{\delta}b}\right]$$
$$=\frac{(h_i+\delta_1)}{2}f(x_i)+\frac{k_1\delta_2\bar{\delta}f(x_{i+1/2})}{k_2\delta_1+k_1\delta_2+\delta_1\delta_2\bar{\delta}b}+O(\bar{\delta}^2), \tag{12}$$

where $h_i=x_i-x_{i-1}$.

Then, to $O(\bar{\delta}^2)$ we deduce the associated finite difference representation. To identify the equivalent "averaged" coefficients or material properties on interval (x_i, x_{i+1}) we rewrite (12) as

$$-\bar{k}\frac{(u_{i+1}-u_i)}{(x_{i+1}-x_i)}+k_1\frac{(u_i-u_{i-1})}{(x_i-x_{i-1})}+\frac{(x_{i+1}-x_{i-1})}{2}\bar{b}u_i=\frac{(x_{i+1}-x_{i-1})}{2}\bar{f}_i, \tag{13}$$

where

$$\bar{k}=\frac{(x_{i+1}-x_i)\,k_1k_2}{k_2\delta_1+k_1\delta_2+\delta_1\delta_2\bar{\delta}b},$$
$$\bar{b}=\frac{b}{(x_{i+1}-x_{i-1})}\left[h_i+\delta_1+\frac{2k_1\delta_2\bar{\delta}}{k_2\delta_1+k_1\delta_2+\delta_1\delta_2\bar{\delta}b}\right],$$
$$\bar{f}_i=\frac{(x_{i+1/2}-x_{i-1})}{(x_{i+1}-x_{i-1})}f_i+\frac{\bar{k}\delta_2 f_{i+1/2}}{k_2(x_{i+1}-x_{i-1})}.$$

For comparison purposes, it is useful to write

$$\bar{f}_i=f_i+f_c, \tag{14}$$

where f_c is a local correction given by

$$f_c=\frac{-\delta_2 f_i}{(x_{i+1}-x_{i-1})}+\frac{\bar{k}\delta_2 f_{i+1/2}}{k_2(x_{i+1}-x_{i-1})}.$$

Similar expressions can be written for the difference equation at node $i+1$ (by inspection).

Clearly, this scheme is formally equivalent to the standard method defined earlier and, hence, incorporates the required flux jump at $\bar{x}=x_{i+1/2}$ to second-order accuracy. Note that the condensation procedure not only influences the choice of mean modulus $\bar{k}$ but also $\bar{b}$ and $\bar{f}$ as shown, and that b enters in $\bar{k}$. In particular, if we consider the case $b=0$, we find

$$\bar{k}=\frac{(\delta_1+\delta_2)\,k_1k_2}{k_2\delta_1+k_1\delta_2} \tag{15}$$

which is the harmonic average, k_H. Moreover, if $b \neq 0$, we can express $\bar{k}$ in (13) alternatively as

$$\bar{k} = k_H/(1+\rho) \sim k_H(1-\rho+O(\rho^2)) \qquad (\rho^2 < 1) \tag{16}$$

with

$$\rho = \delta_1 \delta_2 \bar{\delta} b/(k_2\delta_1 + k_1\delta_2) = O(\delta^2).$$

Note that even if the harmonic average is used, the force term locally at the interface is still modified.

3. Finite Volume Formulation

A similar analysis can be made for difference equations obtained using an integral-based finite volume approach. Let us consider, for simplicity, the case $b=0$ and a "cell" of length h centered at node i with discontinuity interface $\bar{x}$ located at the cell boundary midway between x_i and x_{i+1}. Recalling the expressions in (6) for $\sigma_-(x^*)$ and $\sigma_+(x^*)$, let $\delta_1 = \delta_2 = h/2$ and multiply by $k_+ = k_2$ and $k_- = k_1$, respectively. Setting $x^* = \bar{x}$, adding and simplifying, we obtain

$$\sigma(\bar{x}) = \frac{2k_1k_2}{(k_1+k_2)} \frac{(u(x_i)-u(x_{i+1}))}{h} - \frac{h}{4}\frac{(k_1-k_2)}{(k_1+k_2)} f(\bar{x}) + O(h^2). \tag{17}$$

The flux at $x = x_{i-1/2}$ is simply

$$\sigma(x_{i-1/2}) = k_1 \frac{(u(x_{i-1})-u(x_i))}{h} + k_1 \frac{h^2}{24} u'''(x_{i-1/2}) + O(h^3). \tag{18}$$

In the integral formulation, we set

$$\int_{x_{i-1/2}}^{x_{i+1/2}} -(ku')'\,dx = \sigma(x_{i+1/2}) - \sigma(x_{i-1/2}) = \int_{x_{i-1/2}}^{x_{i+1/2}} f\,dx. \tag{19}$$

Using (17) for $\bar{x} = x_{i+1/2}$ with (18) in (19) and simplifying, we obtain, on setting $\bar{k}$ for the harmonic mean,

$$-\bar{k}\frac{u(x_{i+1})-u(x_i)}{h} + k_1\frac{u(x_i)-u(x_{i-1})}{h} - \frac{h}{4}\left(\frac{k_1-k_2}{k_1+k_2}\right) f(x_{i+1/2})$$
$$= f(x_i)\,h + O(h^2). \tag{20}$$

The difference expression becomes, on setting $f_{i+1/2} = (f_i + f_{i+1})/2 + O(h^2)$,

$$-\bar{k}\frac{(u_{i+1}-u_i)}{h^2} + k_1\frac{(u_i-u_{i-1})}{h^2} = f_i + \frac{1}{8}\left(\frac{k_1-k_2}{k_1+k_2}\right)(f_i+f_{i+1}). \tag{21}$$

Observe again the local correction to the force term that is needed if $k_1 \neq k_2$. This point has been neglected in previous constructions (e.g., see Patankar [11], Aziz and Settari [1]). However, since the difference equation for the grid point at x_{i+1} is also modified by a correction term of equal magnitude but opposite sign, the contribution of the local correction terms to the discrete system is $O(h^2)$. Thus, the effect on the numerical solution is only evident on coarse meshes. However, if the flux at the interface is to be calculated, then the new correction term in (17) may be important. It will be a significant contribution if $f(\bar{x})(k_1 - k_2)$ is not small. Note that, in engineering analysis, it is common practice to calculate $\sigma(\bar{x})$ in the post-processing phase by simply using the harmonic average and divided difference formula, i.e., the first entry on the right in (17). We shall give supporting numerical results in a later section.

4. Two Dimensions

We can extend the analysis directly to higher dimensions. The corresponding elliptic equation is

$$-\mathbf{\nabla} \cdot (k\mathbf{\nabla} u) + bu = f \qquad \text{in} \quad \Omega_1 \cup \Omega_2, \tag{22}$$

where k, b, f are sufficiently regular in Ω_1 and Ω_2 with k discontinuous at the interface Γ of Ω_1, Ω_2. The interface conditions are

$$[\![u]\!] = 0, \qquad [\![k\mathbf{\nabla} u \cdot \mathbf{n}]\!] = 0 \qquad \text{on } \Gamma. \tag{23}$$

Once again, we take $k = k_1$ in Ω_1, $k = k_2$ in Ω_2 with $k_1 \neq k_2$. Let P be any point in the domain and C any straight line through P. Since the Laplacian is rotationally invariant, we can consider (22) in a rotated frame with the y axis parallel to C. Let (x^*, y^*) be the coordinates of P in this frame. Following our previous one-dimensional analysis, we have at P

$$\sigma_x^+ = -k_+ u_x = k_+ \frac{u(x^*, y^*) - u(x^* + \Delta x, y^*)}{\Delta x} + \frac{\Delta x}{2} k_+ u_{xx} + O(\Delta x)^2.$$

Using (22), we rewrite this as

$$\sigma_x^+ = \frac{k_+(u(x^*, y^*) - u(x^* + \Delta x, y^*))}{\Delta x} + \frac{\Delta x}{2}(bu(x^*, y^*) - f(x^*, y^*) - k_+ u_{yy}(x^*, y^*)) + O(\Delta x)^2 \tag{24}$$

and by further Taylor-series approximation for u_{yy},

$$\sigma_x^+ = \frac{k_+(u(x^*, y^*) - u(x^* + \Delta x, y^*))}{\Delta x} + \frac{\Delta x}{2}(bu(x^*, y^*) - f(x^*, y^*))$$
$$- \frac{k_+ \Delta x}{2} \frac{(u(x^*, y^* + \Delta y) - 2u(x^*, y^*) + u(x^*, y^* - \Delta y))}{(\Delta y)^2}$$
$$+ O(\Delta x^2, \Delta x(\Delta y)^2), \tag{25}$$

which yields the desired higher order scheme for computing σ_x^+. Repeating this procedure for σ_x^-, subtracting and simplifying, we obtain, with $\Delta x = \delta_2 > 0$, $\Delta x = -\delta_1 < 0$,

$$[\![\sigma_x]\!] = \frac{k_-}{\delta_1} u(x^* - \delta_1, y^*) - \left(\frac{k_+}{\delta_2} + \frac{k_-}{\delta_1}\right) u(x^*, y^*) + \frac{k_+}{\delta_2} u(x^* + \delta_2, y^*)$$
$$- bu(x^*, y^*) - f(x^*, y^*))\,\delta$$
$$+ \frac{(k_+ \delta_1 + k_- \delta_2)}{2} \frac{(u(x^*, y^* + \Delta y) - 2u(x^*, y^*) + u(x^*, y^* - \Delta y))}{(\Delta y)^2}$$
$$+ O(\delta^2, \delta(\Delta y)^2) \tag{26}$$

and $[\![\sigma_x]\!] = [\![\boldsymbol{\sigma} \cdot \mathbf{n}]\!] = 0$, unit normal $\mathbf{n}$, across line C. We may also deduce directly the desired finite difference scheme at (x^*, y^*) from (26). Here, for simplicity, we have taken Δy constant but retained $\Delta x = -\delta_1, \delta_2$ as in the one-dimensional treatment. If C coincides with the interface Γ, then $k_- = k_1$ and $k_+ = k_2$; otherwise, $k_- = k_+ = k$ and we recover the standard 5-point scheme.

It is common practice to use one-dimensional averaged material coefficients (such as the harmonic mean described earlier) for higher dimensional properties. Our one-dimensional analysis exhibited some of the limitations of this "model" by appealing to local condensation. In higher dimensions, condensation can again be carried out, but not explicitly at the local grid-point level. Condensation now corresponds to block partitioning to separate nodal values on the interface and simultaneous preelimination of all these values (see also MacKinnon and Carey [9]). One can, however, develop an approximate representation as follows:

Let $(x^*, y^*) = (x_{i+1/2}, y_j)$ be on Γ and $x_{i+1/2} = x_i + \delta_1 = x_{i+1} - \delta_2$. Then (24) becomes

$$\sigma_x^+ = k_2 \frac{u(x_{i+1/2}, y_j) - u(x_{i+1}, y_j)}{\delta_2} + \frac{\delta_2}{2}(bu(x_{i+1/2}, y_j) - f(x_{i+1/2}, y_j))$$
$$- \frac{\delta_2}{2} k_2 u_{yy}(x_{i+1/2}, y_j) + O(\delta^2) \tag{27}$$

and

$$[\![\sigma_x]\!] = \frac{k_1}{\delta_1} u(x_i, y_j) - \left(\frac{k_2}{\delta_2} + \frac{k_1}{\delta_1}\right) u(x_{i+1/2}, y_j) + \frac{k_2}{\delta_2} u(x_{i+1}, y_j)$$
$$- (bu(x_{i+1/2}, y_j - f(x_{i+1/2}, y_j))\,\bar{\delta}$$
$$+ \frac{(k_2\delta_2 + k_1\delta_1)}{2}(u_{yy}(x_{i+1/2}, y_j)) + O(\delta^2) = 0. \tag{28}$$

Using this, we can solve for the interface value *implicitly* in

$$u(x_{i+1/2}, y_j) = \left(\frac{k_2}{\delta_2} + \frac{k_1}{\delta_1} + b\bar{\delta}\right)^{-1} \left[\frac{k_1}{\delta_1} u(x_i, y_j) + \frac{k_2}{\delta_2} u(x_{i+1}, y_j)\right.$$
$$\left. + f(x_{i+1/2}, y_j)\,\bar{\delta} + \frac{(k_2\delta_2 + k_1\delta_1)}{2} u_{yy}(x_{i+1/2}, y_j)\right] + O(\delta^2). \tag{29}$$

If $u_{yy} = 0$, the problem degenerates to the one-dimensional case studied earlier, and we may use the modified coefficients $\bar{k}$, $\bar{b}$, and $\bar{f}$ obtained by condensation in the previous analysis. If $u_{yy} \neq 0$, then using the above implicit relation and condensing this "pseudo-one-dimensional" case, we may derive an implicit relation for the condensed system at node i,

$$\frac{-k_1k_2(u(x_{i+1}, y_j) - u(x_i, y_j))}{k_2\delta_1 + k_1\delta_2 + \delta_1\delta_2\,\bar{\delta}b} + \frac{k_1}{h_i}(u(x_i, y_j) - u(x_{i-1}, y_j))$$
$$+ \left[\frac{h_i + \delta_1}{2} + \frac{k_1\delta_2\bar{\delta}}{k_1\delta_2 + k_2\delta_1 + \delta_1\delta_2\,\bar{\delta}b}\right] bu(x_i, y_j) - \frac{(h_i + \delta_1)}{2} k_1 u_{yy}(x_i, y_j)$$
$$= \frac{(h_i + \delta_1)}{2} f(x_i, y_j) + \frac{k_1\delta_2}{(k_2\delta_1 + k_1\delta_2 + \delta_1\delta_2\,\bar{\delta}b)}$$
$$\times \left(f(x_{i+1/2}, y_j)\,\bar{\delta} + \frac{(k_1\delta_1 + k_2\delta_2)}{2} u_{yy}(x_{i+1/2}, y_j)\right) + O(\delta^2). \tag{30}$$

Expanding u_{yy} in a Taylor series about (x_i, y_j),

$$u_{yy}(x_{i+1/2}, y_j) = u_{yy}(x_i, y_j) + \delta_1 u_{yyx}(x_i, y_j) + O(\delta_1^2)$$

so that $u_{yy}|_{i+1/2}^{j} \sim u_{yy}|_i^j$ to $O(\delta_1)$ and we have the approximate representation

$$\frac{-k_1k_2(u(x_{i+1}, y_j) - u(x_i, y_j))}{k_2\delta_1 + k_1\delta_2 + \delta_1\delta_2\,\bar{\delta}b}$$
$$+ \frac{k_1}{h_i}(u(x_i, y_j) - u(x_{i-1}, y_j))$$

$$+\left[\frac{h_i+\delta_1}{2}+\frac{k_1\delta_2\delta}{2}+\frac{k_1\delta_2\bar{\delta}}{k_1\delta_2+k_2\delta_1+\delta_1\delta_2\,\bar{\delta}b}\right]bu(x_i, y_j)$$

$$-\left[\frac{(h_i+\delta_1)}{2}k_1+\frac{k_1\delta_2}{(k_2\delta_1+k_1\delta_2+\delta_1\delta_2\,\bar{\delta}b)}\frac{(k_1\delta_1+k_2\delta_2)}{2}\right]$$

$$\times\frac{(u(x_i, y_{j+1})-2u(x_i, y_j)+u(x_i, y_{j-1}))}{(\Delta y)^2}=\frac{(h_i+\delta_1)}{2}f(x_i, y_j)$$

$$+\frac{k_1\delta_2\bar{\delta}}{(k_2\delta_1+k_1\delta_2+\delta_1\delta_2\,\bar{\delta}b)}f(x_{i+1/2}, y_j)+O(\delta^2, \delta(\Delta y)^2). \tag{31}$$

For $b=0$, $\delta_1=\delta_2=h/2$, $\Delta x=\Delta y=h$ we get, to $O(h^2)$, the finite difference formula

$$\frac{-\bar{k}}{h}(u^j_{i+1}-u^j_i)+\frac{k_1}{h}(u^j_i-u^j_{i-1})+k_1\frac{(u^{j+1}_i-2u^j_i+u^{j-1}_i)}{h}$$

$$=\frac{3h}{4}f_i+\frac{1}{4}\frac{\bar{k}}{k_2}hf^j_{i+1/2}. \tag{32}$$

Remark. From the above derivations, we see that two correction terms now enter—one for the force term $f_{i+1/2}$ and the second due to $u_{yy}(x_{i+1/2}, y_j)$. The correction due to u_{yy} at $x_{i+1/2}$ is $O(\delta^2)$ and, hence, will not be significant except on coarse meshes and if $|u_{yyx}|$ is large at x_i. The correction term $f_{i+1/2}$ enters in the same manner as in the one-dimensional case and also will be significant only on very coarse meshes.

In the finite volume approach, let us for simplicity consider the case $b=0$ with cell C_{ij} centered at (x_i, y_j) so that

$$\int_\Omega f\,dx=\int_\Omega -\nabla\cdot(k\nabla u)\,dx=\sum_{C_{ij}}\int_{\partial C_{ij}}-k\nabla u\cdot\mathbf{n}\,ds=\sum_{C_{ij}}\int_{\partial C_{ij}}\boldsymbol{\sigma}^i\cdot\mathbf{n}\,ds. \tag{33}$$

For cell C_{ij} using 1-point Gauss quadratures, we have

$$f^j_i h^2=[\sigma_x|^j_{i+1/2}-\sigma_x|^j_{i-1/2}+\sigma_y|^{j+1/2}_i-\sigma_y|^{j-1/2}_i]\,h+O(h^2). \tag{34}$$

Following the same procedure as in the one-dimensional case, we can write

$$\sigma_x|^j_{i+1/2}=\frac{2k_1k_2}{(k_1+k_2)}\frac{(u^j_i-u^j_{i+1})}{h}-\frac{h}{4}\left(\frac{k_1-k_2}{k_1+k_2}\right)f^j_{i+1/2}+O(h^2)$$

$$\sigma_x|^j_{i-1/2}=k_1\frac{(u^j_{i-1}-u^j_i)}{h}+O(h^2)$$

and so on. Using these expressions in (34), we have the discrete approximation

$$f_i^j h = \frac{-2k_1k_2}{(k_1+k_2)}\frac{(u_{i+1}^j - u_i^j)}{h} + k_1\frac{(u_i^j - u_{i-1}^j)}{h}$$
$$+ \frac{k_1}{h}(u_i^{j+1} - 2u_i^j + u_i^{j-1}) - \frac{h}{4}\left(\frac{k_1-k_2}{k_1+k_2}\right)f_{i+1/2}^j$$

as before. Again, the method is equivalent to the previous approach and the same observations apply.

5. Numerical Results

In the first numerical study, we compare numerical results for a model two-point problem using the harmonic mean with and without the correction term to the source function. The model problem defined in (1)–(2) is considered on (0, 1) with homogeneous Dirichlet boundary data $u(0)=0$, $u(1)=0$ and parameter values: $b=0$, $f=1$. We consider two sets of material modulus values $k_1=0.1$, $k_2=1.0$ and $k_1=0.1$, $k_2=10.0$. The material discontinuity is located at $\bar{x}=0.5$. The analytic solution to this problem is

$$u(x) = \begin{cases} a_1\dfrac{x^2}{2} + b_1 x & 0 \leqslant x \leqslant \frac{1}{2} \\ a_2\dfrac{x^2}{2} + b_2 x + c_2 & \frac{1}{2} \leqslant x \leqslant 1, \end{cases}$$

where $a_i = -1/k_i$, $b_1 = -\frac{1}{4}(3a_2 + a_1)(k_2/(k_2+k_1))$, $b_2 = (k_1/k_2)\,b_1$ and $c_2 = -(b_2 + a_2/2)$.

Since all derivatives of the analytic solution higher than u'' are zero, the approximate difference equation (9) is exact and equal to its analytic representation (8). Therefore, it follows that the finite difference solution to (1) using (13) is *exact* at the nodes. However, when we neglect the source function correction term in (14), the local accuracy of the approximation near $\bar{x}$ is degraded and the resulting finite difference solution is no longer exact at the nodes.

To examine the effect of neglecting the source function correction term, we conducted a series of computations on uniformy refined meshes. In Fig. 1, we plot discrete maximum error norms $\|\mathbf{e}\|_\infty$, as a function of mesh size h on a log–log scale where $\mathbf{e}$ is the vector of grid point error values. The error has been normalized by the maximum analytic solution value. The error converges to zero at a rate of 2 (slope of curves) and the magnitude of the error is significant for the coarser meshes only. Also, accuracy decreases as the contrast between k_1 and k_2 increases. Examining this latter point in more detail, consider the source function correction term f_c for a uniform mesh and constant f

$$f_c = \frac{1}{4}\left(\frac{R-1}{R+1}\right)f,$$

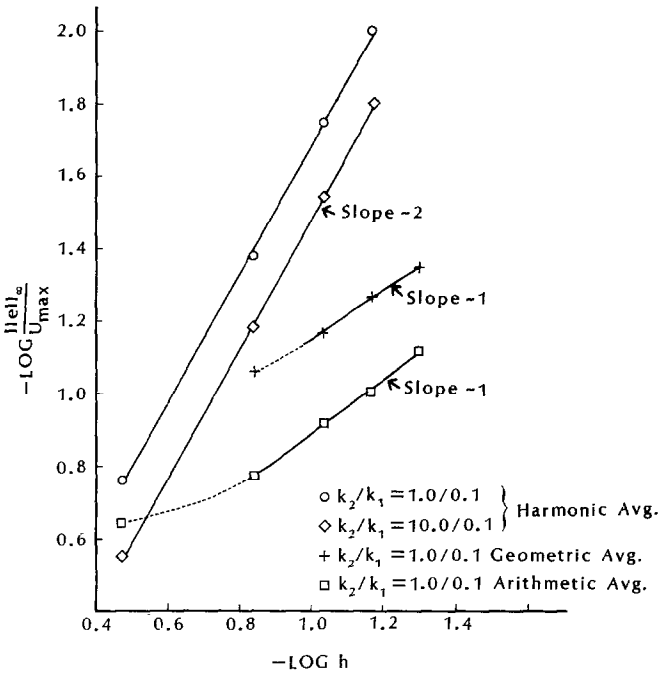

FIG. 1. Rates of convergence in the maximum norm for various averages and uniform mesh refinement.

where

$$R = k_1/k_2.$$

As R ranges from zero to infinity, f_c varies between $-\frac{1}{4}f$ to $\frac{1}{4}f$.

For comparison, we conducted a series of mesh refinement computations using the geometric and arithmetic means with $k_1 = 0.1$, $k_2 = 1.0$. Normalized error norms are plotted in Fig. 1. The errors are significantly larger than those computed using the harmonic mean. Furthermore, convergence rates of unity are obtained and are suboptimal. The discrete L^2 norm of the error behaves similarly.

We also examined rates of convergence in the continuous L^2 norm as the mesh is refined. In Fig. 2, errors in the L^2 norm $\|e\|_0 = \{\int e^2\, dx\}^{1/2}$, where $e = u - u_h$ for exact solution u and piecewise linear interpolant u_h (as in finite-element analysis) of the approximate solution vector **u**, are plotted for both sets of material modulus values, including and excluding the source function correction term. Results of similar accuracy and a convergence rate (slope 1.5) of $O(h^{1.5})$ are obtained, with and without the source correction term. We also plot results for the case where we place a node on the interface and $k_1 = 0.1$, $k_2 = 1.0$. A rate of convergence is determined by slope 2 to be $O(h^2)$. The suboptimal rate of 1.5 in the first instance is

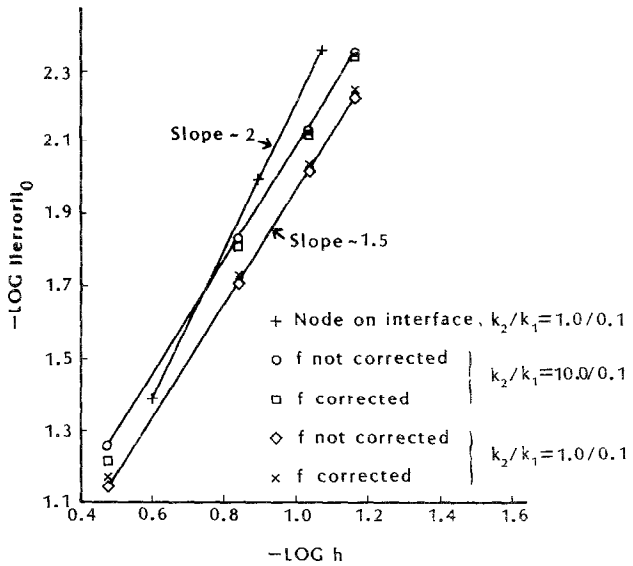

FIG. 2. Rates of convergence (slope) in the L^2 norm and uniform mesh refinement.

caused by the fact that linear interpolation is enforced across the interval containing the interface.

In the next set of numerical studies for this problem, we computed fluxes at the material interface, for $k_1 = 0.1$, $k_2 = 1.0$. Results obtained using (13) and (17) are presented in Table I for the flux σ^*, computed including source correction terms, and σ_h obtained by neglecting source correction terms. The value of σ^* is exact since the analytic solution is quadratic. The flux σ_h is not exact, errors being $O(h^2)$ but significant only on the coarsest mesh ($h = \frac{1}{3}$).

Finally, we compute rates of convergence for the flux obtained using the improved formula (5). We consider the case $k_1 = k_2 = 1$, $b = 1$, and $f = x$ with $u(0) = u(1) = 0$, which was the subject of similar finite element studies (Carey [4]). Rates of convergence for the flux error at boundary $x = 1$ and interior node point $x = 0.5$ are given in Table II, and the post-processing formula is verified to be second-order accurate.

TABLE I

Fluxes σ^* and σ_h Evaluated at $x = 0.5$; $\sigma_{\text{exact}} = 0.204545$

h	σ^*	σ_h	$\lvert\sigma_h - \sigma_{\text{exact}}\rvert$
1/3	0.204545	0.181818	0.022727
1/7	0.204545	0.200372	0.004173
1/11	0.204545	0.202854	0.001691
1/15	0.204545	0.203971	0.000911
			(rate ~ 2)

TABLE II

Flux Errors for the Case $k_1 = k_2 = 1$ and $b = 1$ Evaluated at $x = 0.5$ and $x = 1.0$

h	$e(0.5)$	$e(1.0)$
1/4	0.010180	0.009541
1/8	0.002549	0.002388
1/16	0.000638	0.000599
	(rate ~ 2)	(rate ~ 2)

Two-Dimensional Studies

First, we compare results for a problem using the harmonic mean and the condensation approach (nodes on the interface). The model problem defined in (22)–(23) is considered on $(0, 1) \times (0, 1)$ for $b = f = 0$ with specified boundary data

$$u = \begin{cases} 400x(1-x), & y = 0, \quad 0 < x < 1 \\ 0, & \text{otherwise,} \end{cases}$$

and material ratios $k_2/k_1 = 10, 100$. The analytic solution to this problem is given in MacKinnon and Carey [9].

The error in the discrete maximum norm is plotted against mesh size h in a log–log plot for uniform mesh refinement in Fig. 3. A convergence rate of 2 is

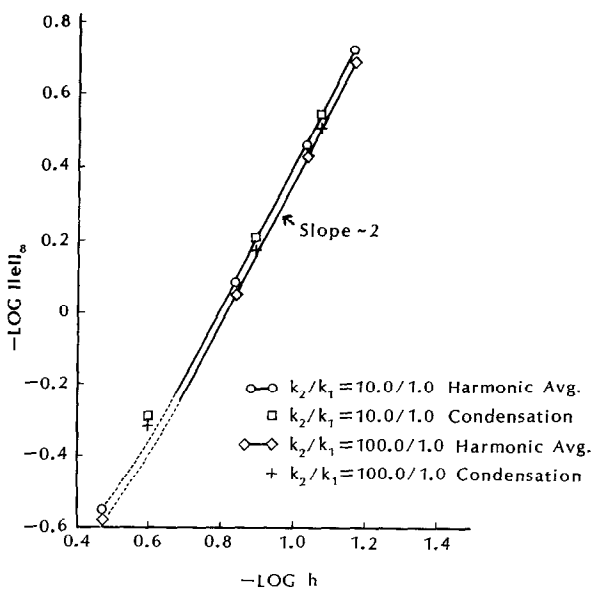

FIG. 3. Rates of convergence in the maximum norm using the harmonic mean and condensation.

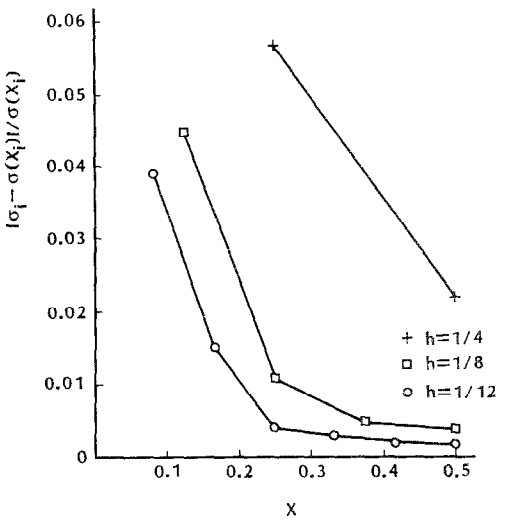

FIG. 4. Interpolant of relative error in flux normal to boundary $y=0$, $0<x<1$, for three mesh refinements $h=\frac{1}{4}, \frac{1}{8}, \frac{1}{12}$ (left half shown).

obtained with the error relatively insensitive to material contrast. Results given by the condensation approach are slightly more accurate for the coarser meshes with both methods yielding the same accuracy on moderate meshes.

Remark. Recall that the correction term due to the second derivative of u in the direction parallel to the interface is $O(h^2)$ and is significant only on coarser meshes.

In our final numerical study, we examine the accuracy of boundary flux approximations given by the finite difference analogs to (25). Relative errors in successive approximations along the side $y=0$, $0<x<0.5$ for $k_2/k_1=10$ are shown in Fig. 4. Since the solution u is symmetric about $x=0.5$, we plot fluxes for $x<0.5$ only. Also, the corner flux $\sigma_y(0,0)$ is not plotted since it is given exactly by the specified boundary data. The figure shows that accuracy decreases as the corner is approached, but relative errors are still quite small. This behavior was observed in similar studies for finite element computations (Carey *et al.* [5]). Nodal errors on the boundary do converge at the optimal rate (Table III).

TABLE III

Flux Errors for Successive Meshes

h	$e(0.0, 0.25)$	$e(0.0, 0.5)$
1/4	13.1	5.98
1/8	2.60	1.15
1/12	0.996	0.505
	(rate ~ 2)	(rate ~ 2)

6. Concluding Remarks

A detailed analysis of finite difference models for treating a material discontinuity interface has been developed. This leads to a modified form of the harmonic average for accommodating the discontinuity. We show that on coarse meshes and under certain conditions the new correction terms are needed but that, with only slight refinement, the contribution of these terms falls dramatically and the simple harmonic average suffices.

Furthermore, this analysis has led to the development of a post-processing scheme for computing nodal fluxes to high accuracy. This scheme is particularly useful in instances where the primary aim of the finite-difference analysis is to obtain accurate fluxes (stresses).

It should be emphasized that the results presented here are for a single rectilinear interface in a specified direction; however, they can be applied to a finite number of mutually orthogonal interfaces, provided the mesh size is sufficiently small and that the analysis is extended to treat the intersection of two interfaces. The problem of "averaging" on a coarser scale would necessitate the inclusion of multiple correction terms which would again become unimportant if subscale grids are used.

APPENDIX 1: Higher Order Flux Formulas

If b is constant, repeated differentiations of (1) implies $-ku^{(n+2)}+bu^{(n)}=f^{(n)}$ and hence

$$\sigma(x^*)=\frac{k[u(x^*)-u(x^*+\delta)]}{\delta}+\frac{\delta}{2}(bu(x^*)-f(x^*))+\frac{\delta^2}{3!}(bu'(x^*)-f'(x^*))$$
$$+\cdots+\frac{\delta^{n+1}}{(n+2)!}(bu^{(n)}(x^*)-f^{(n)}(x^*))+O(\delta^{n+2}). \tag{A.1}$$

If $b=0$, this expansion can be used directly. For $b\neq 0$, the odd derivatives u', u''' must be estimated. For example, we may use the expansion (A.1) rewritten as

$$-u'=\frac{\sigma}{k}=\frac{u(x^*)-u(x^*+\delta)}{\delta}+\frac{\delta}{2k}(bu(x^*)-f(x^*))+O(\delta^2).$$

and substitute in (A.1) to obtain

$$\sigma(x^*)=\frac{k[u(x^*)-u(x^*+\delta)]}{\delta}+\frac{\delta}{2}(bu(x^*)-f(x^*))$$
$$-\frac{\delta^2}{3!}\left[b\frac{(u(x^*)-u(x^*+\delta))}{\delta}+f'(x^*)\right]+O(\delta^3)$$

and so on.

Remark. Similar results can be obtained when k is not constant by writing (1) as $ku'' = bu - f - k'u'$ so that instead of (5) we have

$$\sigma(x^*) = \frac{k[u(x^*) - u(x^* + \delta)]}{\delta} + \frac{\delta}{2}\left(b(x^*)\, u(x^*) - f(x^*) + \frac{k'\sigma(x^*)}{k}\right) + O(\delta^2)$$

or

$$\left(1 - \frac{\delta k'}{2k}\right)\sigma(x^*) = \frac{k[u(x^*) - u(x^* + \delta)]}{\delta} + \frac{\delta}{2}\left(b(x^*)\, u(x^*) - f(x^*)\right) + O(\delta^2)$$

so that

$$\sigma(x^*) = \left(1 - \frac{\delta k'}{2k}\right)^{-1}\left[\frac{k[u(x^*) - u(x^* + \delta)]}{\delta} + \frac{\delta}{2}\left(b(x^*)\, u(x^*) - f(x^*)\right)\right] + O(\delta^2).$$

In summary, we see that flux formulas of arbitrary order can be generated in this manner at the "expense" of function and derivative evaluations of f, b, and k at x^*.

REFERENCES

1. K. AZIZ AND A. SETTARI, *Petroleum Reservoir Simulation* (Applied Science Publ., Ltd., London, 1979), p. 83.
2. I. BABUSKA, *Computing* **5**, 207 (1970).
3. J. H. BRAMBLE AND B. E. HUBBARD, *Contribs. to Diff. Eqs.* **3**, 399 (1964).
4. G. F. CAREY, *J. Comput. Meth. Appl. Mech. Eng.* **35**, 1 (1982).
5. G. F. CAREY, S. S. CHOW, AND M. SEAGER, *J. Comput. Meth. Appl. Mech. Eng.* **50**, 107 (1985).
6. G. F. CAREY AND J. T. ODEN, *Finite Elements: Computational Aspects* (Prentice–Hall, Englewood Cliffs, NJ, 1983), p. 173.
7. G. F. CAREY AND J. T. ODEN, *Finite Elements: A Second Course* (Prentice–Hall, Englewood Cliffs, NJ, 1983), p. 221.
8. T. DUPONT, *SIAM J. Numer. Anal.* **13**, 362 (1976).
9. R. J. MACKINNON AND G. F. CAREY, *Int. J. Numer. Meth. Eng.* **24**, 393 (1987).
10. R. J. MACKINNON AND G. F. CAREY, "Superconvergent Derivatives: A Taylor Series Analysis," 1987 (in preparation).
11. S. V. PATANKAR, *Numerical Heat Transfer and Fluid Flow* (McGraw–Hill, New York, 1980), p. 44.
12. A. N. TIKHONOV AND A. A. SAMARSKII, *USSR Comput. Math. Math. Phys.* **1**, 5 (1962).
13. M. F. WHEELER, *SIAM J. of Numer. Anal.* **11**, 764 (1974).